Journal of Alloys and Compounds 509 (2011) 9884–9889

Contents lists available at ScienceDirect

Journal of Alloys and Compounds

journal homepage: www.elsevier.com/locate/jallcom

Influence of chemical composition and holding time on austenite (γ) → ferrite (α) transformation in ductile iron occurring within the intercritical interval

A. Basso, R. Martínez*, J. Sikora

Facultad de Ingenieria – INTEMA – Universidad Nacional de Mar del Plata – CONICET, Av. Juan B. Justo 4302, B7608FDQ Mar del Plata, Buenos Aires, Argentina

ARTICLE INFO

Article history:
Received 7 February 2011
Received in revised form 20 July 2011
Accepted 21 July 2011
Available online 9 August 2011

Keywords:
Ductile iron
Dual-phase ADI
Matrix microstructure
Allotriomorphic ferrite

ABSTRACT

This work focuses on the influence exerted by the chemical composition on the characteristics of the $\gamma \rightarrow \alpha$ reaction occurring within the intercritical interval of the Fe–C–Si diagram, in order to produce a new "dual phase ADI" variant.

Three ductile iron melts with different chemical compositions were used and several thermal cycles were performed. The results show a strong dependence between the alloy composition and the characteristics of the $\gamma \rightarrow \alpha$ reaction, affecting the amount as well as the morphology of the precipitated allotriomorphic ferrite. Low alloy content promotes ferritic nucleation around graphite nodules and fast growth. Moreover, when the alloy content increases, the ferrite nucleates preferentially at the grain boundaries of the recrystallized austenite, and grows very slowly forming a continuous net. This novel microstructure is expected to enhance the mechanical properties of ductile cast iron.

1. Introduction

During the last decades, ductile iron (DI) production has witnessed a continuous expansion. This fact can be attributed to the improvement achieved in casting technology as well as to the metallurgical advances favouring an increase in the mechanical properties of DI. Further advantages include the possibility of using DI to produce parts of complex geometries and different sizes, providing a more suitable fabrication solution than cast or forged steels [1].

The final microstructure of DI can be conveniently modified by using a wide range of heat treatments (HT), such as ferritizing, normalizing, quenching and tempering, and austempering, obtaining ferritic, pearlitic, martensitic and ausferritic matrices, respectively [2]. Researchers and producers continue in their search for new DI applications, being the safety critical parts market one of their main targets.

In this regard, austempered ductile iron (ADI) and fully ferritic DI are frequently used to produce parts with high toughness and ductility. A new kind of DI is currently under development. It is usually referred to as "dual phase ADI" (or "dual phase"). The matrix of this DI is composed of ausferrite (regular ADI microstructure) and free (or allotriomorphic) ferrite. This combined microstructure can be obtained by subjecting DI to heat treatments comprising an incomplete austenitization step (at temperatures within the intercritical interval of the Fe–C–Si diagram) followed by an austempering stage in a salt bath, in order to transform the austenite into ausferrite [3–6].

This new approach has awoken great technological interest and motivated to focus research efforts on determining and improving the mechanical properties of "dual-phase ADI". Several studies have explored the influence of the relative amount of phases present in the matrix, and the results have demonstrated that it is possible to obtain a wide spectrum of mechanical properties, yielding interesting strength/elongation ratio for certain microstructures, if compared with those of completely ferritic or ausferritic matrices [3–8].

Nevertheless, as of yet the literature has not reported the influence of phase morphology on mechanical properties. Based on previous results [3], the authors of this work have centred on producing "dual phase ADI" by applying new heat treatment cycles, comprising a complete austenitization step followed by a holding stage within the intercritical interval in order to produce the austenite (γ) → ferrite (α) transformation, ending with a final austempering step (Fig. 1). With this new heat treatment cycle a novel microstructure, composed of a fine and continuous network of free ferrite on an ausferritic matrix, can be obtained.

2. Review of concepts on recrystallized and non-recrystallized austenite

In order to explain the morphology displayed by the free ferrite, it is necessary to understand the differences between

* Corresponding author. Tel.: +54 223 4816600x245; fax: +54 223 4810046.
E-mail addresses: abasso@fi.mdp.edu.ar (A. Basso), rimarti@fi.mdp.edu.ar (R. Martínez), jsikora@fi.mdp.edu.ar (J. Sikora).

0925-8388/$ – see front matter © 2011 Elsevier B.V. All rights reserved.
doi:10.1016/j.jallcom.2011.07.069

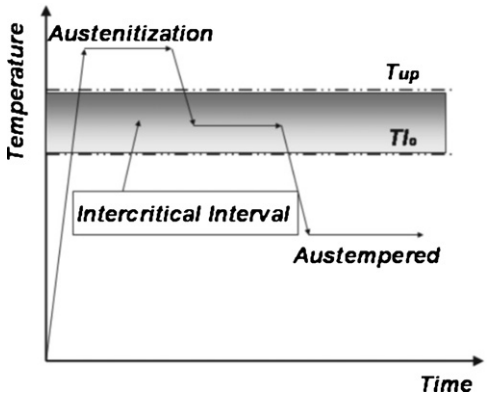

Fig. 1. Heat treatment cycles to obtain "dual phase ADI" [3].

non-recrystallized austenite and recrystallized austenite. This concept has been clearly developed by Sikora and Boeri [9] and Rivera et al. [10]. The cited authors demonstrated the distinct grain size difference existing between the austenite produced during solidification (non-recrystallized austenite) and that obtained after reheating by an austenitizing step (recrystallized austenite). Both kinds of structures are illustrated in Fig. 2.

Fig. 2a depicts the solidification structure of a eutectic DI made up of large solidification austenite grains. These non-recrystallized austenite grains can be revealed by using a special procedure, called Direct Austempering After Solidification (DAAS), developed by Boeri and Sikora [11]. This technique can be applied to every kind of DI, including those of hypereutectic equivalent carbon [10,12]. Fig. 2b is a black and white picture of the results obtained after applying Electro Back Scattering Diffraction (EBSD) to the same DI sample of Fig. 2a, confirming the size and the dendritic characteristics of the non-recrystallized austenite [13].

Fig. 2c, in turn, illustrates the microstructure obtained after reheating a sample composed of the same DI melt as that of Fig. 2a and b, held well above the upper critical temperature, then cooled into the intercritical interval (in order to precipitate the ferrite), and finally water quenched to transform the remaining recrystallized austenite into martensite [3]. An allotriomorphic ferrite network surrounding recrystallized austenite grains (transformed into martensite during quenching) can be clearly observed.

As already described by previous papers [9,14], when non-recrystallized austenite grains transform into ferrite and pearlite during cooling as cast samples, the ferrite precipitates mainly around graphite nodules, exhibiting the well known bull's eye morphology. Nevertheless, the recrystallized austenite obtained during reheating nucleates in a large number of sites in the microstructure, yielding a notoriously lower austenitic grain size, with respect to the noticeable large grains of the austenite produced during solidification (see the scales in Fig. 2a). Then, the recrystallized austenite grain boundaries act as preferential sites for the heterogeneous nucleation of ferrite occurring during the $\gamma \rightarrow \alpha$ solid state transformation within the intercritical interval, allowing obtaining the continuous net of ferrite (Fig. 2c).

Galarreta et al. [15] reported the results of mechanical tests performed on pearlitic matrices containing a continuous net of ferrite. The authors revealed a noticeable enhancement of the mechanical properties in this kind of microstructure, with respect to completely pearlitic matrices, and attributed such an improvement to the fact that the fine ferrite net favours elongation and toughness, leaving strength and hardness almost unaffected.

Taking into account the aspects discussed above, this work focuses on the influence exerted by the chemical composition on the characteristics of the $\gamma \rightarrow \alpha$ reaction occurring within the intercritical interval.

3. Experimental

3.1. Melts and samples

Three ductile iron melts were prepared using a medium frequency induction furnace. Steel scrap and foundry returns were used as raw materials. Nodulization was conducted applying the sandwich method, employing 1.5% of Fe–Si–Mg (6% Mg), while inoculation was performed using 0.6% Fe–Si (75% Si). The melts were poured in 25-mm-thick Y-block-shaped sand moulds. The chemical composition was determined by using a Baird DV6 spectrometer. Round samples of 12 mm diameter and 30 mm length were cut from the Y-blocks and used to prepare test specimens.

3.2. Heat treatments

All the samples employed in the present work were previously ferritised following an annealing heat treatment cycle consisting of:

(i) austenitizing at 910 °C for 3 h.
(ii) cooling down to 740 °C inside the furnace.
(iii) holding at 740 °C for 10 h.
(iv) cooling down to room temperature inside the furnace.

3.2.1. Determination of the intercritical interval

The intercritical interval for each melt was established by employing the methodology described in previous papers by the authors [3,4] which is herein summarized as follows: ferritised specimens were subjected to thermal cycles involving austenitizing stages at temperatures ranging from 720 to 900 °C, at steps of 20 °C. Each complete thermal cycle consisted of holding the sample for 1 h in the furnace at each selected temperature ($T\gamma$). After the heating step, the samples were water quenched. The resulting microstructures were composed of different amounts of ferrite (original matrix) and martensite (quenched austenite). In all cases, the quantification of the relationship between the amounts of ferrite and martensite was carried out using an optical microscope and the Image Pro Plus software. Reported values are the average of at least five determinations on different regions of each sample (evaluated regions were around 1 mm^2). The graphite areas were not considered in the percentage of the reported microconstituents.

It is worth mentioning, according to previous work [3,4], that holding time of about 30 min is enough to reach the equilibrium phase percentages in the $\alpha \rightarrow \gamma$ transformation within the intercritical interval, starting from fully ferritic matrices.

3.2.2. Thermal cycles performed to study the austenite into ferrite transformation

The heat treatment used to study the influence of the chemical composition and the holding time on the $\gamma \rightarrow \alpha$ reaction, involved processing several sets of samples

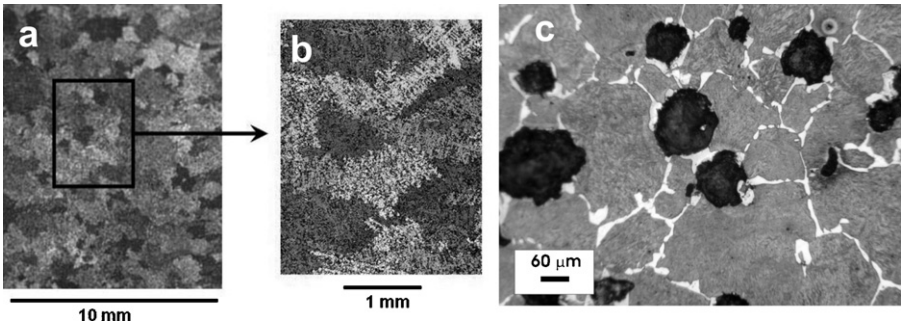

Fig. 2. (a, b) Non-recrystallized austenite and (c) recrystallized austenite [9].

(one set of each melt). This heat treatment was very similar to that shown in Fig. 1. The only difference relies on the water quenching rather than austempering stage at the end of the treatment. The first set of samples was completely austenitized by holding the samples well above the upper critical temperature (910 °C) during 1 h in an electric furnace. Afterwards, they were rapidly transferred to a salt bath at a temperature of 770 °C (temperature within the intercritical interval). This second stage allowed proeutectoid ferrite nucleation and favoured growth on the austenitic matrix ($\gamma \rightarrow \alpha$ reaction). Then, the samples were removed from the salt bath, at one-hour intervals, and water quenched in order to evaluate the evolution of the $\gamma \rightarrow \alpha$ transformation against the holding time through the quantification of the relative amount of martensite and ferrite.

4. Results and discussion

4.1. Characteristics of the materials

The chemical composition of the melts is listed in Table 1. For melt 1, the as-cast microstructure was ferritic–pearlitic and the nodularity exceeded 90%, in accordance with the ASTM A-247 standard. Melts 2 and 3 yielded the same nodularity, though the resulting matrices were completely pearlitic. This difference is ascribed to the higher Cu and Mn contents of these alloys, which promotes pearlite formation and stabilization.

The chemical composition of the melts was decided with a view to assessing the role that the alloying elements, Mn and Cu, play in the $\gamma \rightarrow \alpha$ reaction kinetics in the intercritical interval. As shown in Table 1, Mn and Cu contents increase from melts 1 to 3.

4.2. Intercritical interval

The intercritical interval was determined in agreement with the procedure described in Section 3.2.1. Table 2 lists the amounts (percentages) of ferrite and martensite measured for each sample as a function of the austenitizing temperature (values obtained from $\alpha \rightarrow \gamma$ reaction, starting from a fully ferritic matrix).

As already defined by the authors in previous works [3,4], the lower critical temperature (L_{ct}) is the lower temperature at which the austenite transformation starts (detected by the presence of less than 5% of martensite after quenching). The upper critical temperature (U_{ct}), in turn, is defined as the temperature at which a matrix with over 98% of martensite is detected after quenching the samples held at such temperature. The critical temperature values corresponding to each melt are listed in Table 3. As it is common knowledge, the intercritical interval of DI (critical temperatures and interval amplitude) depends on the chemical composition [16].

Table 1
Melts chemical composition (weight %).

Melt	%C	%Si	%Mn	%Mg	%Cu	%S, P	%CE
1	3.3	2.4	0.2	0.05	0.09	<0.02	4.1
2	3.4	3.0	0.3	0.05	0.99	<0.02	4.4
3	3.3	2.8	0.8	0.04	0.98	<0.02	4.2

Table 2
Relative amounts (percentages) of ferrite (F) and martensite (M) as a function of the austenitizing temperature ($T\gamma$) within the intercritical interval.

$T\gamma$ (°C)	Melt 1	Melt 2	Melt 3
720	100% F	100% F	100% F
740	100% F	100% F	98% F–2% M
760	95% F–5% M	98% F–2% M	85% F–15% M
770	85% F–15% M	95% F–5% M	70% F–30% M
780	75% F–25% M	90% F–10% M	60% F–40% M
800	50% F–50% M	60% F–40% M	30% F–70% M
820	15% F–85% M	20% F–80% M	15% F–85% M
840	5% F–95% M	15% F–85% M	10% F–90% M
860	2% F–98% M	5% F–95% M	5% F–95% M
880	100% M	2% F–98% M	100% M
900	100% M	100% M	100% M

Table 3
Upper and lower critical temperatures of the melts.

Melt	U_{ct} (°C)	L_{ct} (°C)
1	860	750
2	880	760
3	860	740

4.3. Influence of chemical composition and holding time on $\gamma \rightarrow \alpha$ transformation

Fig. 3 illustrates the amount of ferrite present in the microstructure as a function of the holding time at 770 °C, for the three melts analyzed. The ferrite reported values correspond to the amount of ferrite nucleated and growth from a completely austenitic structure ($\gamma \rightarrow \alpha$ reaction within the intercritical interval shown in Fig. 1).

Regarding melt 1, the reaction starts after approximately 15 min. For melt 2, transformation takes about 1 h to start, and it exceeds 2 h for melt 3. The transformation advance is strongly dependent on the chemical composition of the alloy. After holding 9 h at intercritical temperature (770 °C) not any of the heats analyzed in this work reaches the amount of ferrite corresponding to the equilibrium at that intercritical interval temperature (see Table 2). This is a very important difference compared with the transformation time associated to the $\alpha \rightarrow \gamma$ transformation as described previously in Section 3.2.1.

The shape of the curves in Fig. 3 and the amount of ferrite present after 9 h of holding time show that not one of the melts reaches the amount of phases in thermodynamic equilibrium indicated in Table 2. Fig. 3 also evidences the noticeably greater rate of transformation of melt 1 with respect to the other melts. In fact, after holding for 9 h at 770 °C, samples of melt 1 exhibited a microstructure containing about 80% ferrite (α = 85% in equilibrium), while the ferrite content was of about 50% (α = 95% in equilibrium) for samples of melt 2 and below 10% (α = 70% in equilibrium) for melt 3.

The noticeable difference detected in the characteristics of the $\gamma \rightarrow \alpha$ reaction within the intercritical interval can be analyzed by kinetic and thermodynamic factors.

In polymorphous changes that involve nucleation and growth reactions where the parent and product phases have different compositions, such as the $\gamma \rightarrow \alpha$ transformation, there are two successive processes; firstly, long-range transport by diffusion over distances of many atomic spacing, commonly described as the diffusional process. Secondly, atomic transport across the interphase

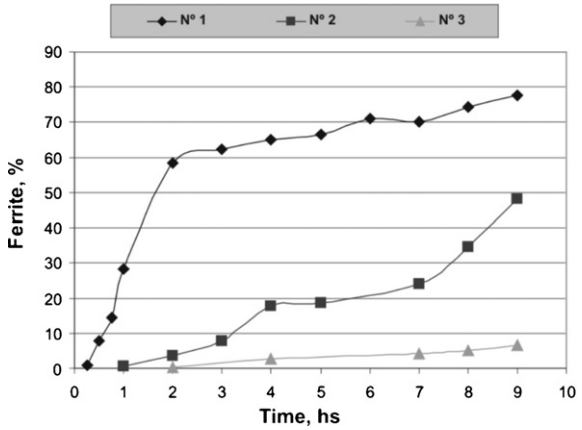

Fig. 3. Amount of ferrite present in the microstructure as a function of the holding time at intercritical temperature for the melts analyzed.

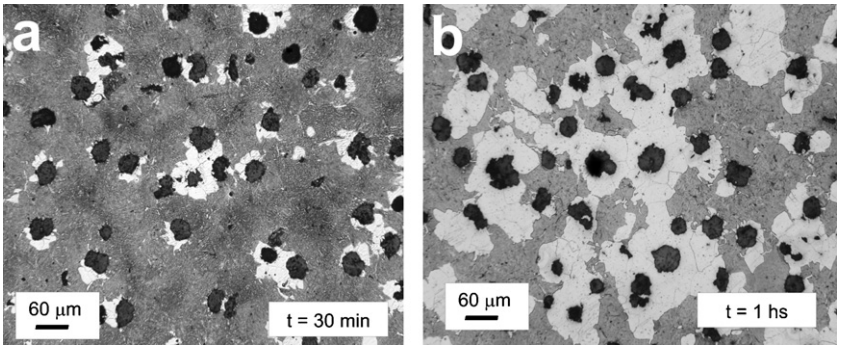

Fig. 4. Transformation $\gamma \rightarrow \alpha$ within the intercritical interval corresponding to melt 1 ($T_{intercritic}$ = 770 °C).

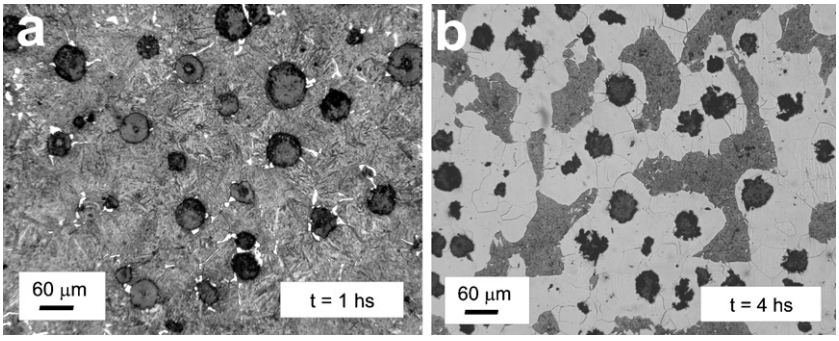

Fig. 5. Transformation $\gamma \rightarrow \alpha$ within the intercritical interval corresponding to melt 2 ($T_{intercritic}$ = 770 °C).

(in this case $\gamma - \alpha$), normally an interfacial thermally activated short-range diffusional process [17]. The long-range diffusion only involves the movements of atoms required to change the composition of the matrix to that of the new phase. In this reaction, carbon atoms must be migrating from the austenite to the graphite nodules. On the other hand, the iron atoms must take part in the interfacial reaction to produce the change in the crystalline structure: γ, fcc $\rightarrow \alpha$, bcc. Since the two processes, long-range diffusion and the short-range interfacial step, are successive reactions, the slower of the two processes will be controlling the transformation rate [17]. Based on these reasons the transformation time of the $\gamma \rightarrow \alpha$ reaction is strongly affected by the chemical composition of the alloy. The addition of chemical elements could change the diffusion rate of the different atomic species, affecting the necessary time to produce both described processes.

Another aspect of relevance is considering that iron substitutional elements (such as Si, Mn and Cu) and their quantities, modify the carbon chemical potential producing changes in the transformation time and phase stability at a given temperature [18].

A more detailed work on these issues should be conducted in order to clarify them, but this is not the aim of this work.

4.4. Influence of chemical composition on phase morphologies

The morphology of the phases present in the microstructure obtained after heat treatment (ferrite and martensite in this case) is another aspect worth considering. Figs. 4–6 show the micrographs corresponding to some points reported on the curves in Fig. 3, for melts 1, 2 and 3, respectively.

For melt 1, ferrite starts to nucleate and grow mainly at the graphite nodule interfaces (Fig. 4a), accounting for an equiaxial growth mode (Fig. 4b), and the zones farther away from the nodule being the last ones to transform. With regard to melt 2, it can be clearly observed that ferrite begins to nucleate and grow not only around graphite nodules but also at the grain boundaries of the recrystallized austenite (Fig. 5b). For melt 3, it is evident that the ferrite nucleates and starts growing mainly at the austenitic grain boundaries (Fig. 6a and b). This change in the characteristics

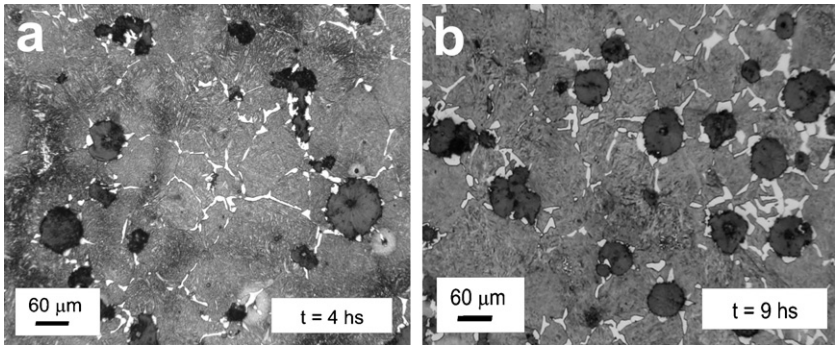

Fig. 6. Transformation $\gamma \rightarrow \alpha$ within the intercritical interval corresponding to melt 3 ($T_{intercritic}$ = 770 °C).

of the $\gamma \rightarrow \alpha$ transformation, and hence in the ferrite morphology for different chemical compositions, is ascribed to the changes in the carbon diffusivity in the metallic matrix, since carbon needs to migrate from the matrix to the graphite nodules to develop the $\gamma \rightarrow \alpha$ reaction, which act as a carbon sink.

For melt 1, with low alloy content, carbon diffusion through the crystalline iron net was relatively easy to achieve, leading to allotriomorphic ferrite formation mainly around the graphite nodules (shorter diffusion path). Notwithstanding the foregoing, as the alloying Fe substitutional element contents increase, the recrystallized austenite grain boundaries act as preferential sites for the heterogeneous nucleation of allotriomorphic ferrite and preferential paths for carbon diffusion, thereby facilitating the growth of ferrite at grain boundaries rather than on the nodule–matrix interfaces.

An aspect worth to analyze is the difference in the holding time necessary to produce the reactions $\alpha \rightarrow \gamma$, and $\gamma \rightarrow \alpha$. The first one is developed at relatively higher rates. In fact, 1 h holding at intercritical autenitizing temperature was enough to reach the equilibrium percentages in the case of the $\alpha \rightarrow \gamma$ transformation, starting from a fully ferritic matrix (see Section 3.2.1 and Table 2). However for the opposite reaction ($\gamma \rightarrow \alpha$ during cooling) several hours at constant temperature were not enough to attain the equilibrium phase percentages (see curves 2 and 3).

This can be related to the fact that in the $\alpha \rightarrow \gamma$ reaction the carbon diffusion necessary to form austenite takes place through this phase, which is the phase that nucleates and grow. In the second case ferrite growth requires that carbon diffuses through this phase to the graphite nodules.

Although the carbon diffusion coefficient in austenite at the temperatures used in this kind of treatments is lower than that of ferrite (two orders of magnitude approximately [19]), the amount of carbon that austenite can dissolve (about 2%) is noticeable larger than that belonging to ferrite (0.02%). Therefore the carbon flux is higher in austenite than in ferrite, causing the differences in transformation rates. It is important to note that ferrite formation requires necessarily that the carbon content goes under 0.02%, while austenite can be formed containing a very wide range of carbon.

4.5. The $\gamma \rightarrow \alpha$ reaction in "dual phase ADI"

As mentioned above, "dual phase ADI" microstructures are composed of different amounts of allotriomorphic ferrite and ausferrite. Given the fact that the goal of this work was to analyze the influence that chemical composition and holding time have on the $\gamma \rightarrow \alpha$ transformation within the intercritical interval, studies were performed on microstructures made up of ferrite and martensite so as to facilitate the experimental methodology. Therefore, the only variant that should be included in the thermal cycle to obtain "dual phase ADI" is samples submission to an austempering stage, rather than water quenching after maintenance at the intercritical temperature (see Fig. 1). This enables austenite → ausferrite transformation instead of the austenite → martensite reaction. Fig. 7 shows the microstructure of an austempered sample at 350 °C.

Taking into account the results reported by Galarreta et al. [15] for pearlitic DI, "dual-phase ADI" matrices are expected to optimize elongation and toughness with respect to conventional completely ausferritic ADI microstructures. This is the main objective of this new line of research currently being undertaken by the authors. On the other hand, emphasis should be placed to improve the manufacturing technology of this new kind of DI, so as to properly select the chemical composition (in order to ease ferrite net formation in periods short enough to be applied in the industrial practice) and to accurately establish the intercritical temperature. If these variables are conveniently selected, the chances of reaching attractive mechanical properties are high.

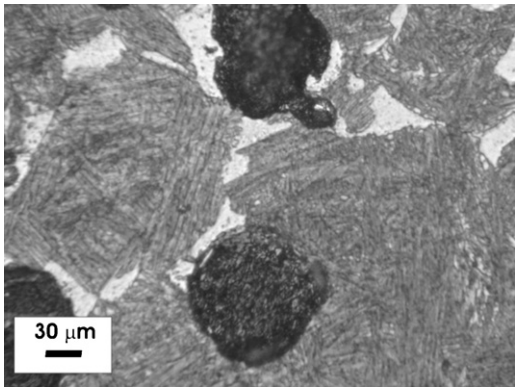

Fig. 7. "Dual phase ADI" microstructure.

5. Conclusions

1. The results obtained in this work display a strong dependence between the characteristic of the $\gamma \rightarrow \alpha$ reaction and the alloy chemical composition.
2. The thermodynamic equilibrium for the $\gamma \rightarrow \alpha$ reaction was not reached after 9 h holdin time in not any of the studied melts.
3. The melt with lower alloying elements (melt 1) begins the $\gamma \rightarrow \alpha$ reaction after 15 min of holding at the intercritical temperature of 770 °C, while that with higher alloy content (melt 3) starts transformation after approximately 2 h.
4. The amount and morphology of the ferrite present in the final microstructure depend on the chemical composition. When alloy content is low, ferrite nucleates and grows around graphite nodules, displaying an equiaxial growth. However if alloy content increases, ferrite nucleates and grows preferentially at the austenite grain boundaries, forming a continuous net of ferrite.
5. From an economic and technical viewpoint, the holding time to develop the $\gamma \rightarrow \alpha$ reaction in the intercritical interval should be short enough to be compatible with industrial practice. The original and promising aspect of the "dual phase ADI" microstructures with a continuous net of ferrite opens new horizons in the study of the mechanical properties of this new type of DI.

Acknowledgments

The financial support granted by CONICET, SECYT and the National University of Mar del Plata is gratefully acknowledged.

References

[1] ASM Handbook, vol. 1: Properties and Selection: Irons and Steel, 9th edition, ASM, United States, 1992, pp. 3–9.
[2] ASM Handbook, vol. 1: Properties and Selection: Irons and Steel, 9th edition, ASM, United States, 1992, pp. 75–96.
[3] A. Basso, R.A. Martínez, J.A. Sikora, Proceedings of the 8th International Symposium on Science and Processing of Cast Iron, Beijing, China, October, Tsinghua University, 2006, pp. 408–413.
[4] A. Basso, R.A. Martínez, J.A. Sikora, Mater. Sci. Technol. 23 (11) (2007) 1321–1326.
[5] V. Kilicli, M. Erdogan, Mater. Sci. Technol. 22 (8) (2006) 919–928.
[6] V. Kilicli, M. Erdogan, Int. J. Cast Met. 20 (4) (2007) 202–214.
[7] J. Aranzabal, G. Serramoglia, C.A. Goria, D. Rousiere, Int. J. Cast Met. Res. 16 (1) (2002) 185–190.
[8] C. Verdu, J. Adrien, A. Reynaud, Int. J. Cast Met. Res. 18 (6) (2005) 346–354.
[9] J. Sikora, R. Boeri, Int. J. Cast Met. Res. 11 (1999) 395–400.
[10] G. Rivera, R. Boeri, J. Sikora, Mater. Sci. Technol. 18 (6) (2002) 691–697.
[11] R. Boeri, J. Sikora, Int. J. Cast Met. Res. 13 (2001) 307–313.

[12] G. Rivera, R. Boeri, J. Sikora, Scripta Mater. 50 (2004) 331–335.
[13] G. Rivera, P.R. Calvillo, R. Boeri, Y. Houbert, J. Sikora, Mater. Charact. 59 (2008) 1342–1348.
[14] R. Boeri, J. Sikora:, ASM Publication of First International Conference on Retained Austenite, 2000, pp. 497–502.
[15] I. Galarreta, R. Boeri, J. Sikora, Int. J. Cast Met. Res. 9 (6) (1997) 353–358.
[16] H.T. Angus:, Cast Iron: Physical and Engineering Properties, 2nd edition, Butterworths, London, 1976.
[17] R. Cahn, Physical Metallurgy, vol. II, 4th edition, 1996 (Chapter 15).
[18] D. Porter, K. Easterling, Phase Transformations in Metals and Alloys, 2nd edition, 1992 (Chapter 2).
[19] C.J. Smithells, Metals Reference Books, 5th edition, 1976.